CERN – SL DIVISION

sumire.tex CERN-SL-2000-003 AP

Computer Calculation of the Transverse Coupling Impedance of Cylindrically Symmetric Structures

H. Tsutsui

Abstract

A new program called “SUMIRE” which calculates the transverse coupling impedance of cylindrically symmetric structures is presented. The method given here is a simple extention of L. Vos’ longitudinal calculation [3].

Geneva, Switzerland

January 28, 2000

Contents

1 Introduction

Longitudinal and transverse coupling impedances are used to estimate the beam instabilities and the heating of the environment. To calculate the coupling impedances of cylindrically symmetric structures, usually ABCI [1] or MAFIA2D [2] time domain simulation codes are used. These codes calculate the wake potentials of some beam distribution, and give the impedances by Fourier transform.

Since the impedance is a notion in frequency domain, it can be calculated directly in this domain. L. Vos [3] wrote a simulation code "CISLIM" in frequency domain for the longitudinal coupling impedance. This program uses field matching techniques to obtain the electromagnetic field inside the structure. For simple structures, CISLIM gives results much faster than ABCI does.

In this report, we extend this method to compute the transverse coupling impedance of cylindrically symmetric structures. The program "SUMIRE" may be used to rapidly obtain estimates of the impedances of such structures. In Section 2, the theory is shown. The theory for the longitudinal impedance is also given in this section. In Section 3, we compare the impedances by our method with those by ABCI for a very simple structure.

2 Theory

The formulae for longitudinal and transverse coupling impedances are given in this section. The theory for longitudinal impedance is already given by L. Vos [3]. Here, we assume: 1) The beam has the velocity of light c, 2) The cross sections are cylindrical, not coaxial, for the sake of simplicity, 3) The radius of the wall changes stepwise, 4) There is no power loss on the wall.

Figure 1 shows an example of the geometry. The radii r_i and the axial distances z_i are defined in this figure.

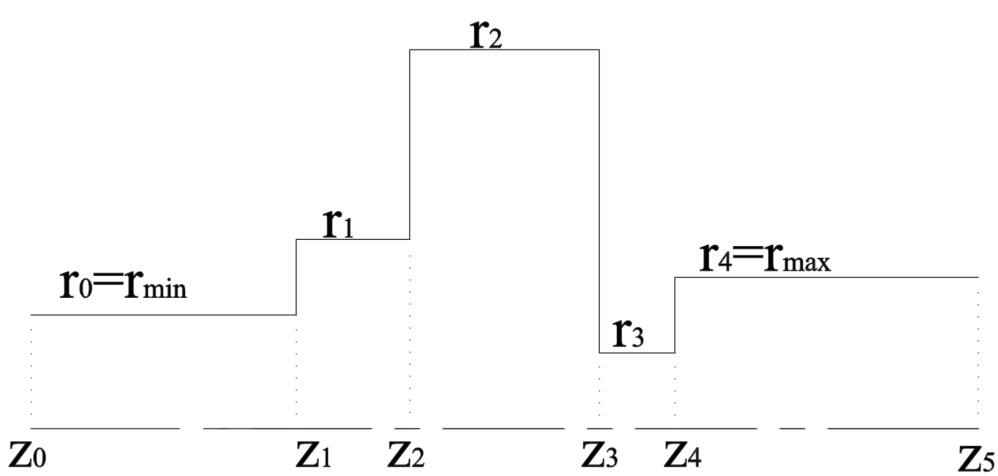

Figure 1: An example of the geometry treated in this report.

2.1 Source Term

Assume an ultra-relativistic pencil beam moving at velocity c along the axial direction z in a pipe of radius a. The charge line density λ of the beam has Fourier components

$$\lambda = \frac{I_0}{c} \exp[j\omega(t - z/c)], \tag{1}$$

where I_0 is the beam current. The time dependence $\exp(j\omega t)$ will be omitted below. We will use the polar coordinate system (r, ϕ, z). When the transverse offset of the beam $(r, \phi) = (\xi, 0)$ is much smaller than a, the electromagnetic field in the pipe is,

$$\begin{aligned} E_r^S &= cB_\phi^S = \frac{\lambda}{2\pi\epsilon_0}\left(\frac{1}{r} + \xi\left(\frac{1}{r^2} + \frac{1}{a^2}\right)\cos\phi\right), \\ E_\phi^S &= -cB_r^S = \frac{\lambda}{2\pi\epsilon_0}\xi\left(\frac{1}{r^2} - \frac{1}{a^2}\right)\sin\phi, \\ E_z^S &= cB_z^S = 0. \end{aligned} \tag{2}$$

The first term of E_r^S is for the monopole mode ($m = 0$), and the others are for the dipole mode ($m = 1$).

2.2 Electromagnetic Waves in the Pipe

For $m = 0$, forward and backward TM0 waves should be considered:

$$\begin{aligned}
E_z^{TM0} &= \sum_{q=0}^{\infty}(F_q^{(0)}\exp(-\gamma_q^{(0)}z) - B_q^{(0)}\exp(\gamma_q^{(0)}z))J_0(z_q^{(0)}r/a), \\
E_r^{TM0} &= \sum_{q=0}^{\infty}(F_q^{(0)}\exp(-\gamma_q^{(0)}z) + B_q^{(0)}\exp(\gamma_q^{(0)}z))\frac{-\gamma_q^{(0)}a}{z_q^{(0)}}J_0'(z_q^{(0)}r/a), \\
E_\phi^{TM0} &= cB_z^{TM0} = cB_r^{TM0} = 0, \\
cB_\phi^{TM0} &= \sum_{q=0}^{\infty}(F_q^{(0)}\exp(-\gamma_q^{(0)}z) - B_q^{(0)}\exp(\gamma_q^{(0)}z))\frac{-jka}{z_q^{(0)}}J_0'(z_q^{(0)}r/a),
\end{aligned} \tag{3}$$

where k and $z_q^{(0)}$ are the wavenumber ($k = \omega/c$) and the q-th zero of the Bessel function J_0 ($J_0(z_q^{(0)}) = 0$), respectively. The propagation constant $\gamma_q^{(0)}$ is

$$\gamma_q^{(0)} = \sqrt{(z_q^{(0)}/a)^2 - k^2}. \tag{4}$$

For $m = 1$, TM1 and TE1 modes should be considered. For the TM1 wave, one has:

$$\begin{aligned}
E_z^{TM1} &= \sum_{q=0}^{\infty}(F_q^{(1)}\exp(-\gamma_q^{(1)}z) - B_q^{(1)}\exp(\gamma_q^{(1)}z))J_1(z_q^{(1)}r/a)\cos\phi, \\
E_r^{TM1} &= \sum_{q=0}^{\infty}(F_q^{(1)}\exp(-\gamma_q^{(1)}z) + B_q^{(1)}\exp(\gamma_q^{(1)}z))\frac{-\gamma_q^{(1)}a}{z_q^{(1)}}J_1'(z_q^{(1)}r/a)\cos\phi, \\
E_\phi^{TM1} &= \sum_{q=0}^{\infty}(F_q^{(1)}\exp(-\gamma_q^{(1)}z) + B_q^{(1)}\exp(\gamma_q^{(1)}z))\frac{\gamma_q^{(1)}a^2}{z_q^{(1)2}}\frac{J_1(z_q^{(1)}r/a)}{r}\sin\phi, \\
cB_z^{TM1} &= 0, \\
cB_r^{TM1} &= \sum_{q=0}^{\infty}(F_q^{(1)}\exp(-\gamma_q^{(1)}z) - B_q^{(1)}\exp(\gamma_q^{(1)}z))\frac{-jka^2}{z_q^{(1)2}}\frac{J_1(z_q^{(1)}r/a)}{r}\sin\phi, \\
cB_\phi^{TM1} &= \sum_{q=0}^{\infty}(F_q^{(1)}\exp(-\gamma_q^{(1)}z) - B_q^{(1)}\exp(\gamma_q^{(1)}z))\frac{-jka}{z_q^{(1)}}J_1'(z_q^{(1)}r/a)\cos\phi,
\end{aligned} \tag{5}$$

where $z_q^{(1)}$ is the q-th zero of the Bessel function J_1 ($J_1(z_q^{(1)}) = 0$). The propagation constant $\gamma_q^{(1)}$ is

$$\gamma_q^{(1)} = \sqrt{(z_q^{(1)}/a)^2 - k^2}. \tag{6}$$

Similarly, for the TE1 wave, the following equations apply:

$$\begin{aligned}
E_z^{TE1} &= 0, \\
E_r^{TE1} &= \sum_{q=0}^{\infty}(F_q^{(1d)}\exp(-\gamma_q^{(1d)}z) + B_q^{(1d)}\exp(\gamma_q^{(1d)}z))\frac{ka^2}{z_q^{(1d)2}}\frac{J_1(z_q^{(1d)}r/a)}{r}\cos\phi, \\
E_\phi^{TE1} &= \sum_{q=0}^{\infty}(F_q^{(1d)}\exp(-\gamma_q^{(1d)}z) + B_q^{(1d)}\exp(\gamma_q^{(1d)}z))\frac{-ka}{z_q^{(1d)}}J_1'(z_q^{(1d)}r/a)\sin\phi, \\
cB_z^{TE1} &= \sum_{q=0}^{\infty}(F_q^{(1d)}\exp(-\gamma_q^{(1d)}z) + B_q^{(1d)}\exp(\gamma_q^{(1d)}z))jJ_1(z_q^{(1d)}r/a)\sin\phi, \\
cB_r^{TE1} &= \sum_{q=0}^{\infty}(F_q^{(1d)}\exp(-\gamma_q^{(1d)}z) - B_q^{(1d)}\exp(\gamma_q^{(1d)}z))\frac{-j\gamma_q^{(1d)}a}{z_q^{(1d)}}J_1'(z_q^{(1d)}r/a)\sin\phi, \\
cB_\phi^{TE1} &= \sum_{q=0}^{\infty}(F_q^{(1d)}\exp(-\gamma_q^{(1d)}z) - B_q^{(1d)}\exp(\gamma_q^{(1d)}z))\frac{-j\gamma_q^{(1d)}a^2}{z_q^{(1d)2}}\frac{J_1(z_q^{(1d)}r/a)}{r}\cos\phi,
\end{aligned} \tag{7}$$

where $z_q^{(1d)}$ is the q-th zero of the first derivative of the Bessel function J_1 ($J_1'(z_q^{(1d)}) = 0$). The propagation constant $\gamma_q^{(1d)}$ is

$$\gamma_q^{(1d)} = \sqrt{(z_q^{(1d)}/a)^2 - k^2}. \tag{8}$$

2.3 Boundary Conditions

When there is a step ($r = a$ to $r = b$ with $a < b$), and regions I and II are on the left and on the right of the step, the following conditions should be applied at the boundary,

$$
\begin{aligned}
E^{TM0}_{I,z}, (0<r<a) &= E^{TM0}_{II,z}, (0<r<a), \\
\left.\begin{array}{ll} E^{S(0)}_{I,r} + E^{TM0}_{I,r}, & (0<r<a) \\ 0, & (a<r<b) \end{array}\right\} &= E^{S(0)}_{II,r} + E^{TM0}_{II,r}, (0<r<b), \\
cB^{S(0)}_{I,\phi} + cB^{TM0}_{I,\phi}, (0<r<a) &= cB^{S(0)}_{II,\phi} + cB^{TM0}_{II,\phi}, (0<r<a), \\
\\
E^{TM1}_{I,z}, (0<r<a) &= E^{TM1}_{II,z}, (0<r<a), \\
\left.\begin{array}{ll} E^{S(1)}_{I,r} + E^{TM1}_{I,r} + E^{TE1}_{I,r}, & (0<r<a) \\ 0, & (a<r<b) \end{array}\right\} &= E^{S(1)}_{II,r} + E^{TM1}_{II,r} + E^{TE1}_{II,r}, (0<r<b), \\
\left.\begin{array}{ll} E^{S(1)}_{I,\phi} + E^{TM1}_{I,\phi} + E^{TE1}_{I,\phi}, & (0<r<a) \\ 0, & (a<r<b) \end{array}\right\} &= E^{S(1)}_{II,\phi} + E^{TM1}_{II,\phi} + E^{TE1}_{II,\phi}, (0<r<b), \\
\left.\begin{array}{ll} cB^{TE1}_{I,z}, & (0<r<a) \\ 0, & (a<r<b) \end{array}\right\} &= cB^{TE1}_{II,z}, (0<r<b), \\
cB^{S(1)}_{I,r} + cB^{TM1}_{I,r} + cB^{TE1}_{I,r}, (0<r<a) &= cB^{S(1)}_{II,r} + cB^{TM1}_{II,r} + cB^{TE1}_{II,r}, (0<r<a), \\
cB^{S(1)}_{I,\phi} + cB^{TM1}_{I,\phi} + cB^{TE1}_{I,\phi}, (0<r<a) &= cB^{S(1)}_{II,\phi} + cB^{TM1}_{II,\phi} + cB^{TE1}_{II,\phi}, (0<r<a).
\end{aligned} \tag{9}
$$

2.4 Field Matching

According to reference [3], we integrate the above equations. For the integration, the following orthogonal relations for different modes of the same wave guide are useful [4]:

$$
\begin{aligned}
\int E_{1,z} E_{2,z} dS = \int \mathbf{E}_{1,t} \cdot \mathbf{E}_{2,t} dS &= 0, \\
\int B_{1,z} B_{2,z} dS = \int \mathbf{B}_{1,t} \cdot \mathbf{B}_{2,t} dS &= 0,
\end{aligned} \tag{10}
$$

where $\mathbf{E}_t$ and $\mathbf{B}_t$ are the transverse vectors of the electric and the magnetic fields, respectively. Some formulae for the integration are given in Appendix A.

2.4.1 Longitudinal ($m = 0$) Case

From the continuity of E_z, we obtain,

$$
\begin{aligned}
(F^{(0)}_{I,p} \exp(-\gamma^{(0)}_{I,p} z) - B^{(0)}_{I,p} \exp(\gamma^{(0)}_{I,p} z)) &= \sum_{q=0}^{\infty} G_{p,q} (F^{(0)}_{II,q} \exp(-\gamma^{(0)}_{II,q} z) - B^{(0)}_{II,q} \exp(\gamma^{(0)}_{II,q} z)), \\
G_{p,q} &= \frac{2 z^{(0)}_p}{a^2 J_1(z^{(0)}_p)} \frac{J_0(z^{(0)}_q a/b)}{(z^{(0)}_p/a)^2 - (z^{(0)}_q/b)^2}.
\end{aligned} \tag{11}
$$

These equations correspond to the integrations of E_z with r from 0 to a with the weight of $J_0(z^{(0)}_p r/a)$. Since the set of functions $\{J_0(z^{(0)}_p r/a)\}$ is a complete orthogonal system, these integrals have enough information for the continuity of E_z.

Similarly, from the continuity of E_r, we obtain,

$$
\begin{aligned}
\sum_{q=0}^{\infty} H_{p,q} \gamma^{(0)}_{I,q} (F^{(0)}_{I,q} \exp(-\gamma^{(0)}_{I,q} z) + B^{(0)}_{I,q} \exp(\gamma^{(0)}_{I,q} z)) &= \gamma^{(0)}_{II,p} (F^{(0)}_{II,p} \exp(-\gamma^{(0)}_{II,p} z) + B^{(0)}_{II,p} \exp(\gamma^{(0)}_{II,p} z)) - C0_p, \\
H_{p,q} &= \frac{2 z^{(0)2}_p a^2 J_1(z^{(0)}_q)}{z^{(0)}_q b^4 J_1^2(z^{(0)}_p)} \frac{J_0(z^{(0)}_p a/b)}{(z^{(0)}_q/a)^2 - (z^{(0)}_p/b)^2}, \\
C0_p &= -\frac{\lambda}{\pi \epsilon_0 b^2} \frac{J_0(z^{(0)}_p a/b)}{J_1^2(z^{(0)}_p)}.
\end{aligned} \tag{12}
$$

When $a > b$, we obtain the equations by exchanging $a \leftrightarrow b$ and $I \leftrightarrow II$.

2.4.2 Transverse ($m = 1$) Case

From the continuity of E_z, we obtain,

$$
\begin{aligned}
(F_{I,p}^{(1)} \exp(-\gamma_{I,p}^{(1)} z) - B_{I,p}^{(1)} \exp(\gamma_{I,p}^{(1)} z)) &= \sum_{q=0}^{\infty} P_{p,q} (F_{II,q}^{(1)} \exp(-\gamma_{II,q}^{(1)} z) - B_{II,q}^{(1)} \exp(\gamma_{II,q}^{(1)} z)), \\
P_{p,q} &= \frac{2 z_p^{(1)}}{a^2 J_0(z_p^{(1)})} \frac{J_1(z_q^{(1)} a/b)}{(z_q^{(1)}/b)^2 - (z_p^{(1)}/a)^2}.
\end{aligned} \tag{13}
$$

From the continuity of cB_z, we obtain,

$$
\sum_{q=0}^{\infty} Q_{p,q} (F_{I,q}^{(1d)} \exp(-\gamma_{I,q}^{(1d)} z) + B_{I,q}^{(1d)} \exp(\gamma_{I,q}^{(1d)} z)) = (F_{II,p}^{(1d)} \exp(-\gamma_{II,p}^{(1d)} z) + B_{II,p}^{(1d)} \exp(\gamma_{II,p}^{(1d)} z)),
$$

$$
Q_{p,q} = \frac{2 z_p^{(1d)} z_q^{(1d)} a J_0(z_q^{(1d)})}{[z_p^{(1d)2} - 1] b^3 J_0^2(z_p^{(1d)})} \frac{J_1'(z_p^{(1d)} a/b)}{(z_q^{(1d)}/a)^2 - (z_p^{(1d)}/b)^2}. \tag{14}
$$

By using the continuity of E_r, E_ϕ and the orthogonality relation, we obtain,

$$
\sum_{q=0}^{\infty} R_{p,q} \gamma_{I,q}^{(1)} (F_{I,q}^{(1)} \exp(-\gamma_{I,q}^{(1)} z) + B_{I,q}^{(1)} \exp(\gamma_{I,q}^{(1)} z)) + \sum_{q=0}^{\infty} S_{p,q} \gamma_{I,q}^{(1d)} (F_{I,q}^{(1d)} \exp(-\gamma_{I,q}^{(1d)} z) + B_{I,q}^{(1d)} \exp(\gamma_{I,q}^{(1d)} z)) =
$$
$$
\gamma_{II,p}^{(1)} (F_{II,p}^{(1)} \exp(-\gamma_{II,p}^{(1)} z) + B_{II,p}^{(1)} \exp(\gamma_{II,p}^{(1)} z)) - C1_p,
$$

$$
\begin{aligned}
R_{p,q} &= \frac{2 z_p^{(1)2} a^2 J_0(z_q^{(1)})}{z_q^{(1)} b^4 J_0^2(z_p^{(1)})} \frac{J_1(z_p^{(1)} a/b)}{(z_p^{(1)}/b)^2 - (z_q^{(1)}/a)^2}, \\
S_{p,q} &= -\frac{2 k a^2 J_0(z_q^{(1d)}) J_1(z_p^{(1)} a/b)}{z_q^{(1d)} b^2 J_0^2(z_p^{(1)})}, \\
C1_p &= -\frac{2\lambda\xi}{\pi\epsilon_0 a b^2} \frac{J_1(z_p^{(1)} a/b)}{J_0^2(z_p^{(1)})}.
\end{aligned} \tag{15}
$$

By using the continuity of cB_r, cB_ϕ and the orthogonality relation, we obtain,

$$
\gamma_{I,p}^{(1d)} (F_{I,p}^{(1d)} \exp(-\gamma_{I,p}^{(1d)} z) - B_{I,p}^{(1d)} \exp(\gamma_{I,p}^{(1d)} z)) - C2_p =
$$
$$
\sum_{q=0}^{\infty} T_{p,q} \gamma_{II,q}^{(1d)} (F_{II,q}^{(1d)} \exp(-\gamma_{II,q}^{(1d)} z) - B_{II,q}^{(1d)} \exp(\gamma_{II,q}^{(1d)} z)) + \sum_{q=0}^{\infty} U_{p,q} \gamma_{I,q}^{(1)} (F_{I,q}^{(1)} \exp(-\gamma_{I,q}^{(1)} z) - B_{I,q}^{(1d)} \exp(\gamma_{I,q}^{(1)} z)),
$$

$$
\begin{aligned}
T_{p,q} &= \frac{2 z_p^{(1d)3} b}{[z_p^{(1d)2} - 1] z_q^{(1d)} a^3 J_0(z_p^{(1d)})} \frac{J_1'(z_q^{(1d)} a/b)}{(z_p^{(1d)}/a)^2 - (z_q^{(1d)}/b)^2}, \\
U_{p,q} &= \frac{2 k z_p^{(1d)} b^2 J_1(z_q^{(1)} a/b)}{[z_p^{(1d)2} - 1] z_q^{(1)2} a^2 J_0(z_p^{(1d)})}, \\
C2_p &= -j \frac{\lambda z_p^{(1d)} \xi}{\pi\epsilon_0 [z_p^{(1d)2} - 1] a J_0(z_p^{(1d)})} \left(\frac{1}{a^2} - \frac{1}{b^2} \right).
\end{aligned} \tag{16}
$$

When $a > b$, we obtain the equations by exchanging $a \leftrightarrow b$ and $I \leftrightarrow II$.

2.5 Impedance

2.5.1 Longitudinal ($m = 0$) Impedance

The induced voltage $V_\parallel$ can be calculated as:

$$
V_\parallel = \int_{-\infty}^{\infty} dz E_z^{TM0}(r = 0, \phi, z; t = z/c) = \int_{-\infty}^{\infty} dz E_z^{TM0}(r = 0, \phi, z) \exp(jkz). \tag{17}
$$

The longitudinal impedance $Z_\parallel$ is defined as

$$\begin{aligned} Z_\parallel &= \frac{-V_\parallel}{I_0} \\ &= -\sum_i \sum_{p=0}^{\infty} \left[F_{i,p}^{(0)} \frac{\exp((-\gamma_{i,p}^{(0)}+jk)z_{i+1}) - \exp((-\gamma_{i,p}^{(0)}+jk)z_i)}{-\gamma_{i,p}^{(0)}+jk} \right. \\ &\quad \left. -B_{i,p}^{(0)} \frac{\exp((\gamma_{i,p}^{(0)}+jk)z_{i+1}) - \exp((\gamma_{i,p}^{(0)}+jk)z_i)}{\gamma_{i,p}^{(0)}+jk} \right], \end{aligned} \tag{18}$$

By using

$$\frac{\partial E_z \exp(jkz)}{\partial r} = \frac{\partial (E_r + cB_\phi)\exp(jkz)}{\partial z}, \tag{19}$$

the above expression can be modified to

$$\begin{aligned} Z_\parallel = & \sum_i \sum_{p=0}^{\infty} \frac{jkr_i^2}{z_p^{(0)2}} \left[F_{i,p}^{(0)} [\exp((-\gamma_{i,p}^{(0)}+jk)z_{i+1}) - \exp((-\gamma_{i,p}^{(0)}+jk)z_i)] \right. \\ & \left. -B_{i,p}^{(0)} [\exp((\gamma_{i,p}^{(0)}+jk)z_{i+1}) - \exp((\gamma_{i,p}^{(0)}+jk)z_i)] \right] + \frac{1}{2\pi\epsilon_0 c} \log \frac{r_{out}}{r_{in}}. \end{aligned} \tag{20}$$

This formula is more useful than Eq. (18) because of the better convergence ($z_p^{(0)}, \gamma_p^{(0)} \propto p$ for large p).

2.5.2 Transverse ($m = 1$) Impedance

The transverse impedance $Z_\perp$ is given by

$$\begin{aligned} Z_\perp &= \frac{j}{I_0 \xi} \int_{-\infty}^{\infty} dz (E_x(r=0,\phi,z) - cB_y(r=0,\phi,z)) \exp(jkz) \\ &= \sum_i \sum_{p=0}^{\infty} \frac{jr_i}{2z_p^{(1)}} \left[F_{i,p}^{(1)} [\exp((-\gamma_{i,p}^{(1)}+jk)z_{i+1}) - \exp((-\gamma_{i,p}^{(1)}+jk)z_i)] \right. \\ &\quad \left. -B_{i,p}^{(1)} [\exp((\gamma_{i,p}^{(1)}+jk)z_{i+1}) - \exp((\gamma_{i,p}^{(1)}+jk)z_i)] \right] \\ &\quad + \sum_i \sum_{p=0}^{\infty} \frac{r_i}{2z_p^{(1d)}} \left[F_{i,p}^{(1d)} [\exp((-\gamma_{i,p}^{(1d)}+jk)z_{i+1}) - \exp((-\gamma_{i,p}^{(1d)}+jk)z_i)] \right. \\ &\quad \left. +B_{i,p}^{(1d)} [\exp((\gamma_{i,p}^{(1d)}+jk)z_{i+1}) - \exp((\gamma_{i,p}^{(1d)}+jk)z_i)] \right]. \end{aligned} \tag{21}$$

This formula has slower convergence than for the longitudinal case because the coefficients $jr_i/2z_p^{(1)}, r_i/2z_p^{(1d)}$ go to zero slowly ($\propto 1/p$).

3 Numerical Evaluation

Equations (20) and (21) truncated to a finite number of modes were implemented in the computer code “SUMIRE”. To check the validity of this model, we compare the results with an ABCI calculation in the case of a simplified structure presented in Figure 2.

Figures 3 and 4 show the longitudinal impedance calculated by this method and by ABCI, respectively. The real part of the longitudinal impedance is zero below cutoff frequency of the TM01 mode (2.295 GHz) because no modes can get out of this small structure. The resonant frequencies correspond to $(2n+1)c/4f \simeq$ 7.5 cm - 5 cm, ($n = 0, 1, 2, \cdots$). There are some gaps which correspond to the cutoff frequencies of the TM0 modes. These two figures have similar but not the same shape. The double peak in Figure 4 is probably an artifact of ABCI.

Figures 5 and 6 show the transverse impedance calculated by this method and by ABCI, respectively. The real part of the transverse impedance is zero below cutoff frequency of the TE11 mode (1.757 GHz) because no modes can get out of this small structure. The quality factor of the resonance around 3 GHz is higher than that for the longitudinal impedance. This may occur when the resonance is between the cutoff frequencies of the TE11 mode (1.757 GHz) and the TM11 mode (3.657 GHz). The imaginary part of the transverse impedance at 0 Hz has a slightly smaller value than with ABCI. This may be due to the convergence problem of this note’s method.

Figures 7 and 8 are convenient to see the convergence at 0 Hz. One may observe that the convergence of the transverse impedance is slower than for the longitudinal case.

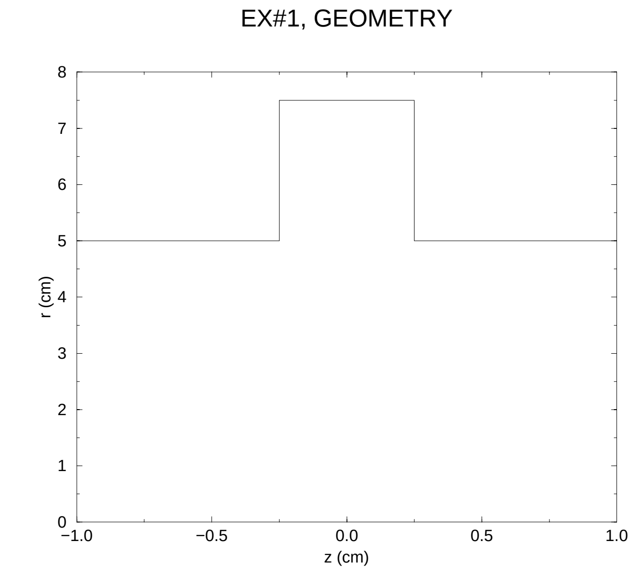

Figure 2: Geometry used for the impedance calculation.

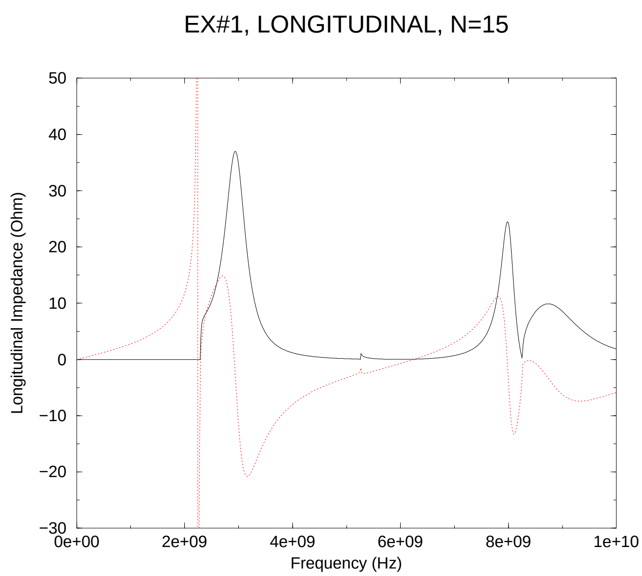

Figure 3: Real part (solid line) and imaginary part (dotted line) of the longitudinal impedance calculated by L. Vos' method. The number of modes is 15.

4 Conclusion

A simple example shows that this method works. But there are some problems: 1) The convergence is not so fast as for the longitudinal case, 2) This program is not for very complicated structures. Maybe a faster algorithm is needed to calculate the transverse impedance of complicated structures.

Acknowledgments

I would like to thank L. Vos and D. Brandt for their encouragement and helpful suggestions. I would like to thank F. Ruggiero for very interesting comments.

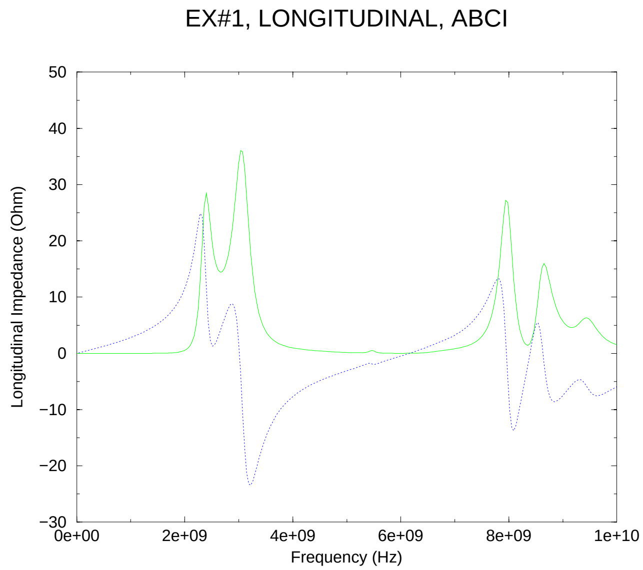

Figure 4: Real part (solid line) and imaginary part (dotted line) of the longitudinal impedance calculated by ABCI.

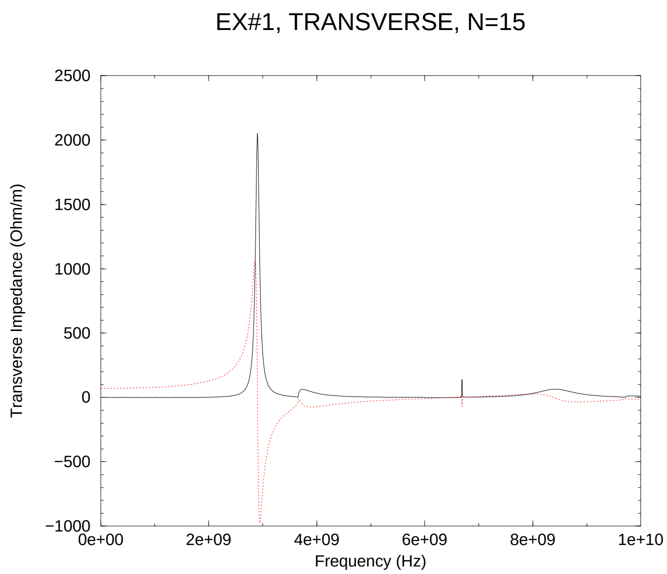

Figure 5: Real part (solid line) and imaginary part (dotted line) of the transverse impedance calculated by this note's method. The number of modes is 2×15.

References

[1] Y.H. Chin, "User's guide for new ABCI : version 6.2 (Azimuthal Beam Cavity Interaction)", CERN SL 92–49 AP rev ESG 216, (1992).

[2] http://www.cst.de

[3] L. Vos, "Computer Calculation of the Longitudinal Impedance of Cylindrically Symmetric Structures and its Application to the SPS", CERN SPS/86–21(MS), (1986).

[4] J.C. Slater, "Microwave Electronics", D. Van Nostrand Co., Inc., (1950).

A Some Useful Integration Formulae

$$J_0'(z) = -J_1(z),$$

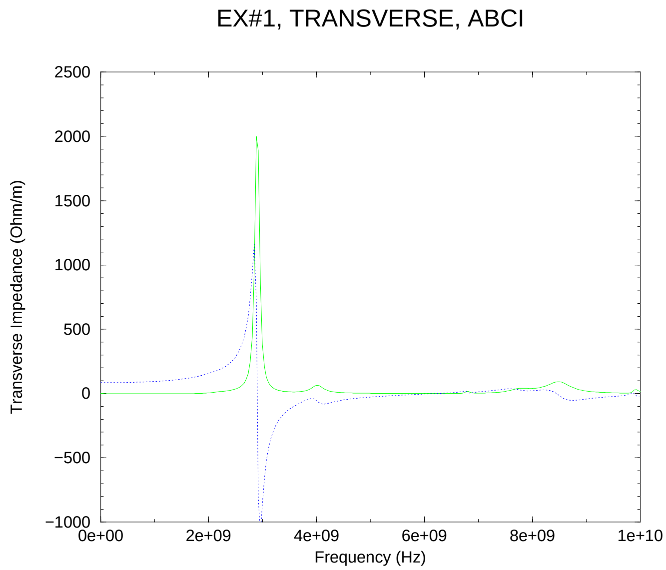

Figure 6: Real part (solid line) and imaginary part (dotted line) of the transverse impedance calculated by ABCI.

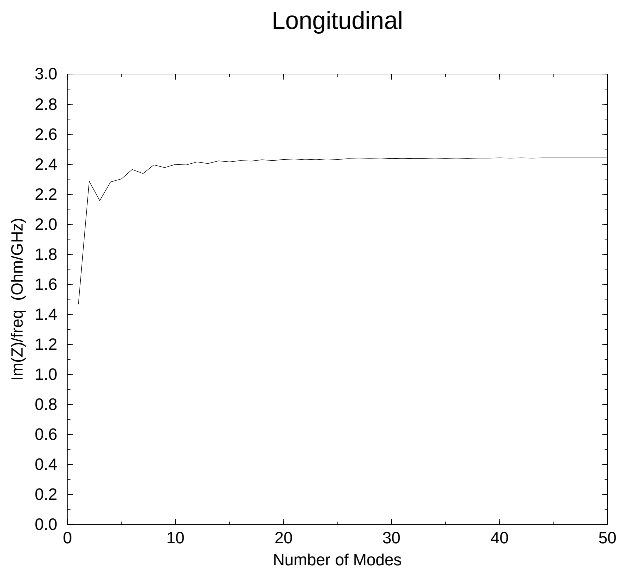

Figure 7: Imaginary part of the longitudinal coupling impedance at 0 Hz vs. the number of modes.

$$\begin{aligned} J_1'(z) &= J_0(z) - J_1(z)/z, \\ J_1''(z) &= (2/z^2 - 1)J_1(z) - J_0(z)/z, \\ J_2(z) &= 2J_1(z)/z - J_0(z), \\ J_1(z_i^{(1d)}) &= z_i^{(1d)} J_0(z_i^{(1d)}), \end{aligned}$$

$$\begin{aligned} \int drr J_p(ar)J_p(br) &= \frac{r}{a^2-b^2}(bJ_p(ar)J_{p-1}(br) - aJ_{p-1}(ar)J_p(br)), \\ \int drr J_p^2(ar) &= \frac{r^2}{2}(J_p^2(ar) - J_{p+1}(ar)J_{p-1}(ar)), \end{aligned}$$

$$\int_0^a drr J_0(z_p^{(0)}r/a)J_0(z_q^{(0)}r/b) = z_p^{(0)} J_1(z_p^{(0)}) \frac{J_0(z_q^{(0)}a/b)}{(z_p^{(0)}/a)^2 - (z_q^{(0)}/b)^2},$$

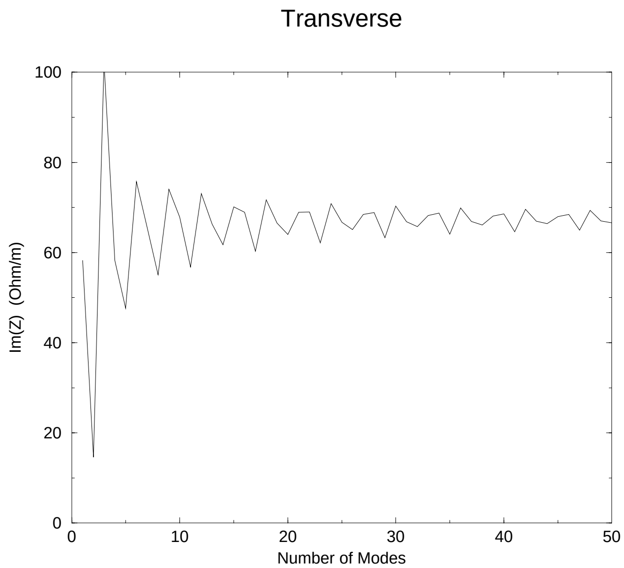

Figure 8: Imaginary part of the transverse coupling impedance at 0 Hz vs. the number of modes.

$$
\begin{aligned}
\int_0^a drr J_0^2(z_p^{(0)} r/a) &= \frac{a^2}{2} J_1^2(z_p^{(0)}), \\
\int_0^a drr J_0'(z_p^{(0)} r/a) J_0'(z_q^{(0)} r/b) &= (z_q^{(0)} a/b) J_1(z_p^{(0)}) \frac{J_0(z_q^{(0)} a/b)}{(z_p^{(0)}/a)^2 - (z_q^{(0)}/b)^2}, \\
\int_0^a drr J_0'^2(z_p^{(0)} r/a) &= \frac{a^2}{2} J_1^2(z_p^{(0)}),
\end{aligned}
$$

$$
\begin{aligned}
\int_0^a drr J_0(z_p^{(1)} r/a) J_0(z_q^{(1)} r/b) &= z_p^{(1)} J_0(z_p^{(1)}) \frac{J_1(z_q^{(1)} a/b)}{(z_q^{(1)}/b)^2 - (z_p^{(1)}/a)^2}, \\
\int_0^a drr J_1^2(z_p^{(1)} r/a) &= \frac{a^2}{2} J_0^2(z_p^{(1)}), \\
\int_0^a drr J_1(z_p^{(1d)} r/a) J_1(z_q^{(1d)} r/b) &= z_p^{(1d)} (z_q^{(1d)} a/b) J_0(z_p^{(1d)}) \frac{J_1'(z_q^{(1d)} a/b)}{(z_p^{(1d)}/a)^2 - (z_q^{(1d)}/b)^2}, \\
\int_0^a drr J_1^2(z_p^{(1d)} r/a) &= \frac{a^2}{2} [z_p^{(1d)2} - 1] J_0^2(z_p^{(1d)}),
\end{aligned}
$$

$$
\begin{aligned}
\int_0^a drr \left[J_1'(z_p^{(1)} r/a) J_1'(z_q^{(1)} r/b) + \frac{a J_1(z_p^{(1)} r/a)}{z_p^{(1)} r} \frac{b J_1(z_q^{(1)} r/b)}{z_q^{(1)} r} \right] &= (z_q^{(1)} a/b) J_0(z_p^{(1)}) \frac{J_1(z_q^{(1)} a/b)}{(z_q^{(1)}/b)^2 - (z_p^{(1)}/a)^2}, \\
\int_0^a drr \left[J_1'^2(z_p^{(1)} r/a) + \frac{a^2 J_1^2(z_p^{(1)} r/a)}{z_p^{(1)2} r^2} \right] &= \frac{a^2}{2} J_0^2(z_p^{(1)}), \\
\int_0^a drr \left[J_1'(z_p^{(1d)} r/a) J_1'(z_q^{(1d)} r/b) + \frac{a J_1(z_p^{(1d)} r/a)}{z_p^{(1d)} r} \frac{b J_1(z_q^{(1d)} r/b)}{z_q^{(1d)} r} \right] &= z_p^{(1d)2} J_0(z_p^{(1d)}) \frac{J_1'(z_q^{(1)} a/b)}{(z_p^{(1d)}/a)^2 - (z_q^{(1d)}/b)^2}, \\
\int_0^a drr \left[J_1'^2(z_p^{(1d)} r/a) + \frac{a^2 J_1^2(z_p^{(1d)} r/a)}{z_p^{(1d)2} r^2} \right] &= \frac{a^2}{2} [z_p^{(1d)2} - 1] J_0^2(z_p^{(1d)}), \\
\int_0^a drr \left[\frac{a}{z_p^{(1d)} r} J_1(z_p^{(1d)} r/a) J_1'(z_q^{(1)} r/b) + \frac{b}{z_q^{(1)} r} J_1'(z_p^{(1d)} r/a) J_1(z_q^{(1)} r/b) \right] &= \frac{ab}{z_q^{(1)}} J_0(z_p^{(1d)}) J_1(z_q^{(1)} a/b),
\end{aligned}
$$

$$
\int_0^a drr \left[J_1'(z_p^{(1)} r/b) + \frac{b}{z_p^{(1)} r} J_1(z_p^{(1)} r/b) \right] = \frac{ab}{z_p^{(1)}} J_1(z_p^{(1)} a/b),
$$

$$\int_a^b dr \left[-\frac{J_1'(z_p^{(1)} r/b)}{r} + \frac{b}{z_p^{(1)} r^2} J_1(z_p^{(1)} r/b) \right] \quad = \quad \frac{b}{z_p^{(1)} a} J_1(z_p^{(1)} a/b),$$